Predicting Object Interactions from Contact Distributions

Oliver Kroemer[1] and Jan Peters[1,2]

***Abstract*— Contacts between objects play an important role in manipulation tasks. Depending on the locations of contacts, different manipulations or interactions can be performed with the object. By observing the contacts between two objects, a robot can learn to detect potential interactions between them.**

Rather than defining a set of features for modeling the contact distributions, we propose a kernel-based approach. The contact points are first modeled using a Gaussian distribution. The similarity between these distributions is computed using a kernel function. The contact distributions are then classified using kernel logistic regression. The proposed approach was used to predict stable grasps of an elongated object, as well as to construct towers out of assorted toy blocks.

I. Introduction

Manipulation tasks almost always involve direct physical contact between two or more objects. These contacts can be between different objects in the robot's environment, or between an object and the robot. Depending on the locations of the contacts, different types of interactions and manipulations can occur. For example, a contact on the side of an object may allow for pushing and sliding the object, while a contact on the bottom can be used for lifting or supporting the object. In order to successfully perform a manipulation task, a robot must be able to determine the potential interactions between objects and utilize them to accomplish the task's goal.

Utilizing contact information in an efficient manner is however not a trivial task. Analytical approaches tend to require accurate models of the objects, and rely on simplified contact models [4]. In an effort to make robots more autonomous, learning approaches have become more widely adopted in the field of robot manipulation [14], [15], [25]. However, representing contacts between objects often relies on hand-crafted features for the given task.

In this paper, we propose an example-based learning approach to detect interactions between objects from their contact distributions. We pose the problem of detecting interactions as a binary classification problem, wherein the robot has to predict whether or not a certain interaction is occurring based on the geometry and relative poses of the objects. The robot first computes which regions of the objects are in contact with each other. The resulting cloud of contact points is subsequently modeled as a Gaussian distribution. A Bhattacharyya kernel function [11] can then be used to compute the similarities between the contact distributions and, thus, classify them using kernel logistic regression. In this manner, the robot uses the similarity between the current contact distribution and previous distributions in order to classify the potential interaction. The details of the approach are explained in Section II.

[1]Oliver Kroemer and Jan Peters are with the Intelligent Autonomous Systems group at the Technische Universitaet Darmstadt, Germany.
[2] Jan Peters is also with the Max Planck Institute for Intelligent Systems.
{kroemer,peters}@ias.tu-darmstadt.de

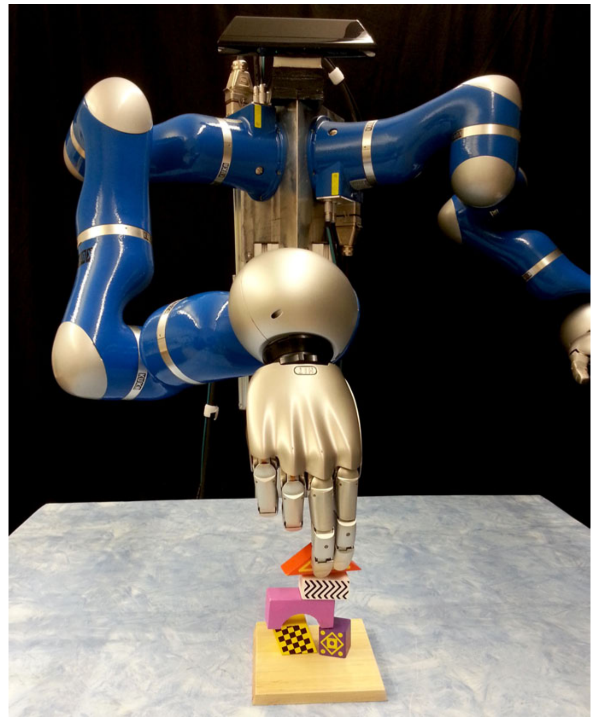

Fig. 1. The Darias robot performing a block stacking task.

The proposed approach was implemented on the real robot shown in Fig. 1. In the first experiment, the robot was given the task of predicting which grasps allow it to steadily pick up an elongated object. The second experiment required the robot to stack assorted blocks. The details of the experiments are given in Section III.

II. Learning From Contact Distributions

In this section, we first outline related work in interaction detection. In Sections II-B to II-D, we explain how contacts between objects are detected and used to create contact distributions. In Sections II-E to II-H, we provide a kernel function for computing the similarity between contact distributions and explain how it is used to classify the distributions using kernel logistic regression.

A. Related Work

Learning symbolic representations of geometric relations between objects, e.g. object A is ON object B, is an important

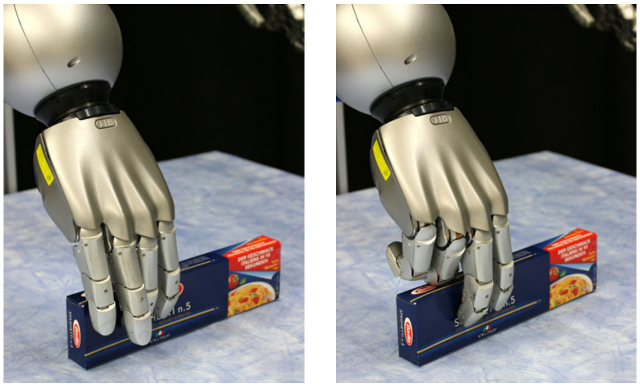

3-Fingered Grasp | 4-Fingered Grasp

Fig. 2. The two types of grasps that were used during the lifting experiment. The three-fingered grasp uses the tips of the thumb, middle, and index fingers in order to pinch the object. The ring and little finger are not touching the box. The four-fingered grasp additionally uses the back of the ring finger on the top of the box in order to provide additional support.

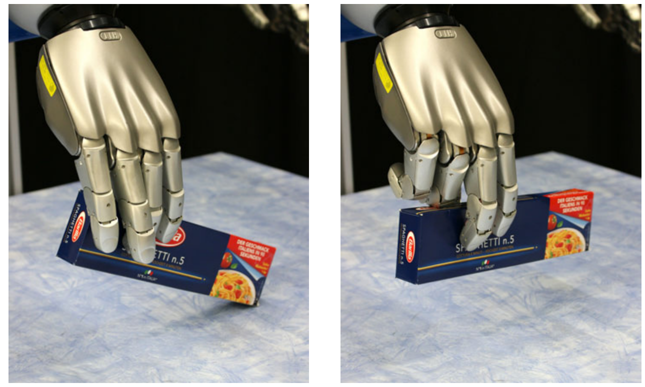

Failed Lift | Successful Lift

Fig. 3. Examples of failed and successful lifts. A lift was considered a failure if the object was still touching the table at the end of the trial.

skill for performing complex manipulation tasks. Rosman and Ramamoorthy [21] proposed the use of a contact network to learn the spatial relations between objects. Contact points were detected using a support vector machine to separate the point clouds of the objects. The vectors between the objects' contact points were then computed and used to classify relations such as *on* and *adjacent* using a k-nearest neighbors classifier. Kulick et al. use an active learning approach to efficiently learn a symbolic representation of the relations between objects [19]. Using features such as the heights of objects and the relative positions between objects, they train a Gaussian process classifier to learn in which geometric states the predicate is true.

Classifying interactions between objects is also closely related to learning affordances [9]. If an object allows a robot to perform an action with it, than the object is said to "afford" that action. Affordances have been widely studied in robotics [23], [16], [20], and especially in the field of robot grasp synthesis [4]. Recently, several papers have proposed template-based approaches for detecting where an object can be grasped [10], [8], [18]. These approaches predict where to grasp an object based on the local shape of the object relative to the hand. The approach presented by Detry et al. [8] learns both the bounding box of points to consider when comparing grasps as well as a dictionary of graspable parts.

Contact information can also be represented in the form of tactile sensor readings. Bekiroglu et al. [1] proposed learning to predict stable grasps of objects using kernel logistic regression. Their approach used a product of three separate kernels based on the position of the hand relative to the object, the approach direction of the hand, and moment features of the tactile sensor arrays' readings. In the work of Dang et al. [7], the locations of the sensed contact points are defined relative to the palm, and modeled using a bag-of-words representation. A support vector machine is then trained to classify stable and unstable grasps.

The features used by learning algorithms can also be designed to capture specific aspects of the contacts between objects. In [25], a classifier was trained on simulated data to predict interactions, such as support and location control, between pairs of objects. The classifier was provided with 93 features, such as the total contact patch area, and the vector between the closest contact point and the other object. Automatic relevance determination was then used to effectively select a subset of these features. Jiang et al. [14] addressed the problem of learning to place objects in a scene. The placement of an object was represented by a set of 145 features, including features for modeling supporting contacts and the caging of objects. A support vector machine with a shared sparsity structure was then used to classify good and bad placements of objects.

B. Contact Points

In order to determine the contacts between objects, we first need a suitable representation of the object and its geometry. Given an object O_i, where i specifies the index of the object, we define its geometry as a point cloud with n_i points at positions $\boldsymbol{p}_{ij}$ and corresponding normals $\boldsymbol{u}_{ij}$ for $j \in \{1, \ldots, n_i\}$. Point clouds are flexible object representations that are widely used in robotics [22]. The normals of the points are straightforward to compute using the covariance of nearby points and the viewing direction.

The point cloud defines the surface of the object and, hence, also where contacts can potentially be made with another object. In order to obtain a set of contact points, each point in the point cloud is classified as either being in contact with the other object or not. In our experiments, we used logistic regression to classify the points, although other methods for detecting contacts are also applicable. The probability of a point $\boldsymbol{p}_{ic}$ being in contact with the object O_j is given by

$$p(\text{contact}|\boldsymbol{p}_{ic}, \boldsymbol{u}_{ic}, O_j) = \left(1 + \exp\left(\boldsymbol{\phi}^T \boldsymbol{\rho}\right)\right)^{-1},$$

where $\boldsymbol{\phi}$ is a vector of feature functions and $\boldsymbol{\rho}$ is a vector of corresponding weights. We used three features, including a density estimation

$$\phi_1(\boldsymbol{p}_{ic}, O_j) = \sum_k \exp\left(-\frac{\left\|\boldsymbol{p}_{ic} - \boldsymbol{p}_{jk}\right\|^2}{\sigma^2}\right)$$

and a surface normal density estimation

$$\phi_2(\boldsymbol{p}_{ic}, \boldsymbol{u}_{ic}, O_j) = \sum_k (\boldsymbol{u}_{ic}^T \boldsymbol{u}_{jk}) \exp\left(-\frac{\left\|\boldsymbol{p}_{ic} - \boldsymbol{p}_{jk}\right\|^2}{\sigma^2}\right)$$

where σ is the length scale of the density. We also include a bias term $\phi_3 = 1$.

These three features are well-suited for detecting arbitrary contacts between two objects. Some interactions however require specific types of contacts, e.g., cutting requires contact with a sharp edge. The set of features can be easily extended for more specific types of contacts.

Computing a set of weights $\boldsymbol{\rho}$ that maximizes the likelihood of the training data is a convex optimization problem, and can be solved using iterative reweighted least squares, as explained in [2]. A point is classified as a contact point if the probability of contact is greater than 0.5.

C. Object Centers

In addition to the shape of the object, we also define a set of *object centers* for each object. Object centers are used to define interaction-relevant coordinate frames for the object. Each center $\boldsymbol{c}_{ik}$, where k is the index of the center for object O_i, is associated with a position $\boldsymbol{x}_{ik}$ and at least one axis $\boldsymbol{a}_{ik}$. For example, the position of an object's center of gravity is given by the mean point of its mass, and an axis pointing down in the direction of gravity. For an articulated object, such as a hand winch or door handle, the position and axis of rotation of the revolute joint defines another center. Although an object may have many centers, usually only one center is used for predicting an interaction. In this paper, we only consider a single object center $\boldsymbol{c}_i$, and leave automatically selecting the relevant center to future work.

Once the contact points have been found, they need to be defined with respect to the center's coordinate frame. If the axes of the center already defines three orthogonal axes $\boldsymbol{a}_i^x$, $\boldsymbol{a}_i^y$, and $\boldsymbol{a}_i^z$ this step is trivial. However, the center of gravity or the center of a revolute joint only define a single axis $\boldsymbol{a}_i^x$ and not a full 3D coordinate frame. In order to define the other two axes, we first project the contact points into a 2D plane, with the normal of the plane given by the first axis of the center $\boldsymbol{a}_i^x$. We then compute the matrix of second moments about the center position for the contact points, and subsequently compute the eigenvectors of the matrix. The second axis $\boldsymbol{a}_i^y$ is defined by the eigenvector with the largest eigenvalue, such that the mean of the contact points is in the positive direction. Using this approach, the contact point clouds are aligned according to the radial direction with the largest variance. The third axis is simply given by the cross product of the first two $\boldsymbol{a}_i^z = \boldsymbol{a}_i^x \times \boldsymbol{a}_i^y$.

The positions of the $\tilde{n}_i$ contact points in the object center's coordinate frame are denoted as $\tilde{\boldsymbol{p}}_{ij}$ with corresponding normals $\tilde{\boldsymbol{u}}_{ij}$ for $j \in \{1, \ldots, \tilde{n}_i\}$.

D. Computing Contact Distributions

Having computed a set of contact points, we now want to compare this set of contacts to previously observed ones. Rather than comparing points individually, we first model the set of contact points as a distribution. In particular, we model them as a 6D Gaussian distribution, where the first three dimensions correspond to the positions of points, and the last three model the normals. In the lifting experiment in Section III, we also investigate replacing the normals of each point with an estimate of the force. However, the forces are in most cases not known, especially when the interaction is between two objects and not with the robot.

Given a set of contacts, we now define a distribution over contact points as a Gaussian distribution. The mean vector $\boldsymbol{\mu}_i$ and variance $\boldsymbol{\Sigma}_i$ of the distribution are given as

$$\boldsymbol{\mu}_i = \frac{1}{\tilde{n}_i} \sum_{k=1}^{\tilde{n}_i} \begin{bmatrix} \tilde{\boldsymbol{p}}_{ik} \\ \tilde{\boldsymbol{u}}_{ik} \end{bmatrix},$$

$$\boldsymbol{\Sigma}_i = \frac{1}{\tilde{n}_i} \sum_{k=1}^{\tilde{n}_i} \left(\begin{bmatrix} \tilde{\boldsymbol{p}}_{ik} \\ \tilde{\boldsymbol{u}}_{ik} \end{bmatrix} - \boldsymbol{\mu}_i \right) \left(\begin{bmatrix} \tilde{\boldsymbol{p}}_{ik} \\ \tilde{\boldsymbol{u}}_{ik} \end{bmatrix} - \boldsymbol{\mu}_i \right)^T.$$

This model provides a compact representation of the mean contact position and normal orientation, as well as the correlations between the parameters around this mean.

E. Kernel Between Contact Distributions

Having converted the contact points into a contact distribution, we can now use a kernel to compute the similarity between distributions. We use the Bhattacharyya kernel [11] which is given by

$$k((\boldsymbol{\mu}_i, \boldsymbol{\Sigma}_i), (\boldsymbol{\mu}_j, \boldsymbol{\Sigma}_j)) = \int \sqrt{\mathcal{N}(\boldsymbol{x}|\boldsymbol{\mu}_i, \boldsymbol{\Sigma}_i)} \sqrt{\mathcal{N}(\boldsymbol{x}|\boldsymbol{\mu}_j, \boldsymbol{\Sigma}_j)} \mathrm{d}\boldsymbol{x}.$$

The computation of the kernel is given in [12], and we include it again here for completeness. The kernel function is computed as

$$k((\boldsymbol{\mu}_i, \boldsymbol{\Sigma}_i), (\boldsymbol{\mu}_j, \boldsymbol{\Sigma}_j)) = C \exp\left(-M/4\right),$$

where the values of C and M are given by

$$C = 0.5^{-d/2} \left|\hat{\boldsymbol{\Sigma}}\right|^{1/2} \left|\boldsymbol{\Sigma}_i\right|^{-1/2} \left|\boldsymbol{\Sigma}_j\right|^{-1/2},$$

$$M = \boldsymbol{\mu}_i^T \boldsymbol{\Sigma}_i^{-1} \boldsymbol{\mu}_i + \boldsymbol{\mu}_j^T \boldsymbol{\Sigma}_j^{-1} \boldsymbol{\mu}_j - \hat{\boldsymbol{\mu}}^T \hat{\boldsymbol{\Sigma}} \hat{\boldsymbol{\mu}}.$$

The vector $\hat{\boldsymbol{\mu}}$ is given by $\hat{\boldsymbol{\mu}} = \boldsymbol{\Sigma}_i^{-1} \boldsymbol{\mu}_i + \boldsymbol{\Sigma}_j^{-1} \boldsymbol{\mu}_j$, and the matrix $\hat{\boldsymbol{\Sigma}}$ is computed as $\hat{\boldsymbol{\Sigma}} = (\boldsymbol{\Sigma}_i^{-1} + \boldsymbol{\Sigma}_j^{-1})^{-1}$. The parameter $d = 6$ is the dimensionality of the Gaussians. The kernel function computes a value from zero to one, where a value of one is achieved if the contact distributions are identical. As the overlap between the distributions decreases, the kernel function tends to zero.

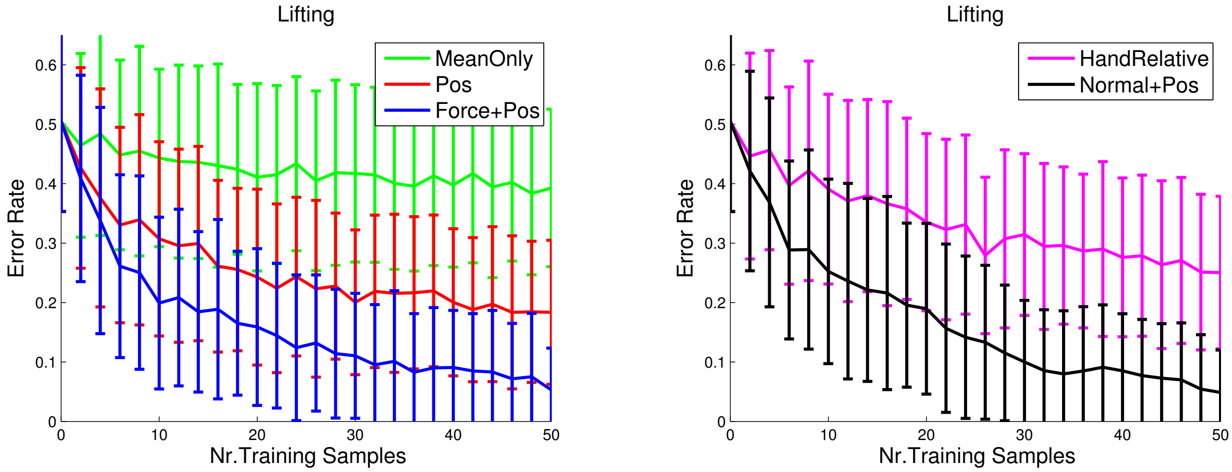

Fig. 4. The expected error rates for the lifting task. The error bars indicate one standard deviation. An error rate of 1 indicates that none of the test samples were correctly classified, and an error rate of 0 is achieved when the classifier evaluates all of the samples correctly.

F. Extension to multiple Gaussians

Although we focus on representing contact distributions using single Gaussians, the proposed framework is straightforward to extend to multiple Gaussians. By representing the contact distribution as a mixture of Gaussians, the model can capture more details of the distribution. The resulting kernel can therefore distinguish between different contact distributions more easily.

However, the Bhattacharyya kernel is not suitable for comparing Gaussian mixture models. Instead, given that the contact distribution of object O_i has the form

$$f_i(\boldsymbol{x}) = \sum_{h=1}^{H_i} \nu_{ih} \mathcal{N}(\boldsymbol{x}|\boldsymbol{\mu}_{ih}, \boldsymbol{\Sigma}_{ih}),$$

where ν_i are the mixture components of the H_i Gaussians, one can compute the kernel function

$$k(f_i(\boldsymbol{x}), f_j(\boldsymbol{x})) = \frac{\int f_i(\boldsymbol{x}) f_j(\boldsymbol{x}) \mathrm{d}x}{\sqrt{\int f_i(\boldsymbol{x}) f_i(\boldsymbol{x}) \mathrm{d}x}\sqrt{\int f_j(\boldsymbol{x}) f_j(\boldsymbol{x}) \mathrm{d}x}},$$

in closed-form. This kernel function also has a value of 1 when the contact distributions are the same, and tends to zero as the overlap decreases. The kernel is based on the expected likelihood kernel [12] and is closely related to the Cauchy-Schwarz divergence [13].

G. Interaction-specific contact similarity

Although the contact distribution is defined in a 6D space, not all of the dimensions will be equally relevant for predicting a given interaction. For example, when pushing open a door, the horizontal distance from the axis of rotation is more relevant than the vertical position along the axis. As a result, two contacts are more similar if they are offset vertically rather than horizontally from each other.

We can model this additional similarity by adding interaction-specific Gaussian noise $\mathcal{N}(\mathbf{0}, \tilde{\boldsymbol{\Sigma}})$ to the contact points. Thus, each contact point is represented as a Gaussian distribution $\mathcal{N}([\ \tilde{\boldsymbol{p}}_{ik}^T \quad \tilde{\boldsymbol{u}}_{ik}^T\ ]^T, \tilde{\boldsymbol{\Sigma}})$ instead of just a single point. If the offset between two contact points corresponds to a direction with a larger variance, then their distributions will overlap more and they will be considered as more similar. In practice, the interaction-specific covariance matrix $\tilde{\boldsymbol{\Sigma}}$ is added to the standard covariance matrices $\boldsymbol{\Sigma}_i$ and $\boldsymbol{\Sigma}_j$ before computing the kernel value. The experiment in Section III-B shows that the robot can use this additional similarity information to increase the sample efficiency of the learning algorithm.

H. Classifying Contact Distributions

Having defined a kernel between contact distributions, we can now use a wide range of kernel methods from machine learning [24]. In order to classify a contact distribution, we use kernel logistic regression. Kernel logistic regression uses the similarity to previously observed distributions, with known labels, to classify new contact distribution. The probability that a contact distribution $\mathcal{N}(\boldsymbol{x}|\boldsymbol{\mu}_i, \boldsymbol{\Sigma}_i)$ allows for a certain interaction $\mathcal{I}$ is given by

$$p(\mathcal{I}|\boldsymbol{\mu}_i, \boldsymbol{\Sigma}_i) = \left(1 + \exp\left(\alpha\right)\right)^{-1},$$

where

$$\alpha = \theta_0 + \sum_{j=1}^{m} \theta_j k((\boldsymbol{\mu}_i, \boldsymbol{\Sigma}_i), (\boldsymbol{\mu}'_j, \boldsymbol{\Sigma}'_j)),$$

and we have m previous examples of contact distributions $\mathcal{N}(\boldsymbol{x}|\boldsymbol{\mu}'_j, \boldsymbol{\Sigma}'_j)$. The weight parameters θ can be learned using iterative reweighted least squares. Contact distributions that are not similar to any previous distributions will have a probability defined by θ_0. As kernel logistic regression is a probabilistic classifier, it can model a contact distribution that only sometimes allows for the interaction. Previous contact distributions that allowed for the interaction will generally have more negative weights, which will result in a probability closer to one.

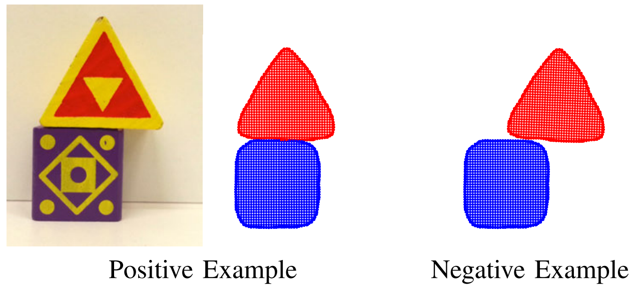

Fig. 5. Point cloud examples of a stable and an unstable stacking of blocks

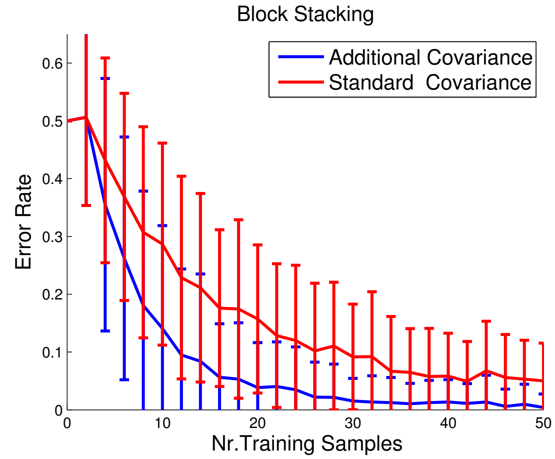

Fig. 6. The expected error rate for the block stacking task. The red line indicates the performance when using the standard covariance matrix. The blue line shows the performance when adding the interaction-specific covariance matrix. The error bars indicate one standard deviation.

III. Experiments

The proposed approach was implemented on a real robot, as shown in Fig. 1. The robot consists of two Kuka lightweight robot arms, each equipped with a DLR five-fingered hand [6], and a kinect. The robot was evaluated on two tasks: picking up an elongated object, and stacking assorted toy blocks.

A. Picking up Elongated Objects

In the first experiment, we applied the framework to the problem of predicting whether a given grasp allows an elongated object to be steadily lifted.

Experimental Setup: The robot performed 60 randomly selected grasps along the length of a spaghetti box. The first half of the grasps were performed with a three-fingered grasp and the other 30 were executed with a four-fingered grasp, as shown in Fig. 2. The robot subsequently tried to lift the box 13 cm above the table. The picking up of the box was considered successful if the object was no longer in contact with the table, and a failure otherwise, as shown in Fig. 3. Before lifting the box, the robot recorded the state of the scene and computed the contact distribution. Based on this information, the robot had to predict whether or not the lift would be successful. In order to detect contact points, we labeled ten points in one scene to train the contact classifier. The contact distribution is defined relative to the center of gravity.

In addition to evaluating the method explained in Section II, referred to here as NORMAL+POS, we also evaluated several benchmark approaches. The first benchmark approach, MEANONLY, performs the classification using only the mean contact $\boldsymbol{\mu}_i$. The POS approach uses only the position distribution of the contact points and not the normals. As a result, the contact distribution is only 3D. Although the fingers do not have tactile sensors, forces can be roughly approximated using the joint torque sensors of the fingers and the relative positions of the contact points. The FORCE+POS approach is the same as NORMAL+POS, except that the normals $\boldsymbol{u}_i$ have been replaced by force estimates. The final method HANDRELATIVE uses the positions and estimated forces of the contact points, but defines the contact distribution relative to the hand rather than the object center.

The performance of the various methods were tested for different numbers for training samples. In each evaluation, ten grasps were selected as test samples. From the remaining grasp samples, a subset of samples were selected as training data. The classifier was then trained on the training data and used to classify the test samples. The error rate is given by the percentage of correctly classified grasps in the test set. This process was repeated 250 times for each classifier and each number of training samples. The results of the evaluation are shown in Fig. 4.

Discussion: Using only the mean contact or the distribution relative to the hand resulted in poor performance. The task was especially challenging for the HANDRELATIVE approach, as the object has the same shape along its length. Despite this challenge, the approach still obtained an error rate of 25.04%.

Using only the position of the contact points relative to the object center resulted in an error rate of 18.36%, which is only marginally better than the performance of HANDRELATIVE. In comparison, the NORMAL+POS and the FORCE+POS achieved error rates of 4.88% and 5.28% respectively. The contact normals clearly capture a considerable amount of information, as they allow side contacts to be differentiated from top contacts.

Both NORMAL+POS and FORCE+POS performed well on the task, and learned to accurately predict steady lifts. However, both approaches also have their limitations. The NORMAL+POS approach cannot differentiate between the robot gently placing its fingers on the box and the fingers applying forces at the contacts. This approach can therefore sometimes only predict whether an interaction is possible, given the contacts, but not if the interaction is being performed. The FORCE+POS approach can differentiate between these two scenarios, and using it together with tactile sensing is a promising direction for future research. However, as the forces between objects will often not be directly observed, the NORMAL+POS approach is generally more applicable.

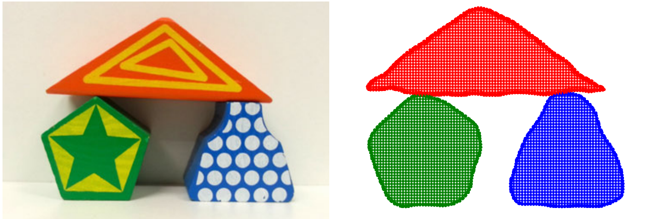

Fig. 7. An example scene with three objects, wherein the green and blue objects are supporting the triangular red block.

Fig. 8. Two examples of block towers constructed by the robot.

B. Stacking Objects

In the second experiment, the robot was given the task of classifying whether one object was supporting another. The robot then used the trained classifier to stack assorted toy blocks.

Classifying Stable Block Placements: The robot was provided with 60 example scenes, each containing two interacting toy blocks, such as the ones shown in Fig. 5. For the 30 negative examples, physically impossible static scenes were created by hand. The models of the blocks were acquired using a turn table setup and a kinect. The object center is again defined by the center of gravity. To train the contact point classifier, ten points were hand labelled in one scene. The points of the object were classified as contacts based on the features described in Section II-B. Using additional features, such as the position and orientation of the points relative to the object's center, were also tested, but had no significant effects on the outcome of the experiment.

The performance of the contact point classifier was evaluated in the same manner as for the previous experiments. A set of ten test samples were randomly selected and removed from the pool of 60 samples. A subset of the remaining samples were then used to train the classifier. The classifier was subsequently applied to the ten test samples, and the error rate was recorded. The error rate is 1 if all ten samples were incorrectly classified, and 0 if all of them were correctly classified. The test samples were subsequently put back into the pool of samples. This process was repeated 250 times for each number of training samples.

In addition to the standard approach, we also evaluated adding an interaction-specific covariance matrix $\tilde{\Sigma}$, as explained in Section II-G. The elements of the diagonal matrix were recomputed for each trial using a basic hill-climbing approach to minimize the leave-one-out cross-validation error rate on the training set.

The results of this experiment are shown in Fig. 6. Starting with error rates close to 50%, the classifiers' performances gradually improves as more samples are provided. Given 50 samples, the standard classifier achieved an expected error rate of 5.0%, and could accurately predict when the object was being supported. Using the additional interaction-specific covariance matrix, the classifier achieved an expected error rate of 0.4% for 50 samples, and only required 20 samples to achieve an expected error rate of 3.84%. The sample efficiency of the algorithm can therefore be increased by incorporating the interaction-specific covariance. In many of the trials, the covariance matrix $\tilde{\Sigma}$ indicated that the vertical position of the supporting contacts was less relevant than the horizontal position. The experiment demonstrates the classifier's ability to generalize between different object shapes.

Generalization to Multiple Objects: In order to demonstrate the classifier's ability to generalize to multiple objects, it was applied to the scene of three objects shown in Fig. 7. In this scene, the top object is being supported by both of the lower objects. When the classifier is applied to the top block and only one of the bottom blocks, the interaction is classified as not supporting. However, we can also combine the blue and green point clouds of the bottom objects in order to create one compound object. When applying the classifier to the top object and this compound object, the top object is labeled as being supported by the bottom object. Thus, as one would expect, the classifier detects that the top is being supported by both objects jointly, and by neither one separately. The classifier was tested on two more similar scenes of three blocks, with the same results.

Building Block Towers: In the final part of the experiment, the real robot used the classifier from the first part to perform block stacking. The interaction-specific covariance matrix was not used in this experiment. The robot was provided with a small wooden board, on which to stack the blocks. In order to avoid all of the blocks being placed directly on the board, the placing of the blocks was limited to a single strip along the middle of the board. For every block, the robot observed the current scene using the kinect and used the resulting point cloud as the supporting object in the interaction. As the focus is not on the planning aspects of the problem, the sequence of blocks was predefined.

In order to determine a suitable placement for the current block, the robot sampled different positions in the scene. For each sample, the contact points were estimated and the probability of the block being supported was computed. The robot then attempted to place the block at the position with the highest probability.

Randomly sampling positions in the scene led to poor performance. One of the main challenges for the robot was the noisy partial point cloud of the current scene. The kinect usually only captured the top and front of the current block stack, but not the back or sides. The lack of reliable points on the sides of objects resulted in unforeseen collisions between blocks. This problem could be alleviated by obtaining more views of the scene, completing the point cloud based on symmetries [3], [17], or applying a penalty for placing the block into occluded regions.

In order to reduce the number of accidental collisions, we also implemented a sampling approach that mimics the movement of the block when it is being put down. The robot sampled 20 horizontal positions at 7.5mm increments across the width of the board. For each horizontal position, the robot sampled vertical placements at 5mm increments in a top-down manner until contact was detected between the block and the stack.

In order to evaluate the proposed approach, the robot was given the task of creating five towers consisting of five blocks each. Using the improved sampling approach, the robot successfully placed 96% of the blocks without knocking any blocks down. Only one block was misplaced by a few millimeters and fell down. The robustness of the system could be further improved by also considering the probability of success of neighboring positions [5].

The robot currently ignores the interactions between blocks further down in the stack. As a result the robot may select a block placement that causes a supporting block to fall down. One potential solution to this problem would be to recheck the interactions between objects further down the stack. For each interaction, the objects higher up in the stack would then be treated as a single compound object, with a corresponding object center. This approach would however require the robot to keep a model of the current scene's geometry.

The results of the experiment show that the robot was able to construct multiple block towers, such as the ones shown in Fig. 8,using the proposed approach. A video of the robot stacking blocks is avaliable at: http://youtu.be/6S5eJgE28sg

IV. Conclusions

In this paper, we presented a kernel-based approach to learning object interactions from contact distributions. The proposed approach is based on modeling the distribution of contact points as a Gaussian distribution. The Bhattacharyya kernel is then used to compute the similarity between the contact distributions. In the experiments, we used kernel logistic regression to predict stable grasps of objects, as well as suitable placements of objects. Using the learned classifier, the robot was able to build small towers out of assorted blocks.

V. Acknowledgments

The research leading to these results has received funding from the European Community's Seventh Framework Programme under grant agreements 610878 (3rdHand), 600716 (CoDyCo), and 610967 (TACMAN).

References

[1] Yasemin Bekiroglu, Renaud Detry, and Danica Kragic. Learning tactile characterizations of object- and pose-specific grasps. In *IEEE/RSJ International Conference on Intelligent Robots and Systems*, 2011.

[2] Christopher M. Bishop. *Pattern Recognition and Machine Learning (Information Science and Statistics)*. Springer-Verlag New York, Inc., Secaucus, NJ, USA, 2006.

[3] J. Bohg, M. Johnson-Roberson, B. León, J. Felip, X. Gratal, N. Bergström, D. Kragic, and A. Morales. Mind the gap - robotic grasping under incomplete observation. In *proceedings of International Conference on Robotics and Automation*, pages 686–693, 2011.

[4] J. Bohg, A. Morales, T. Asfour, and D. Kragic. Data-driven grasp synthesis - a survey. *IEEE Transactions on Robotics*, accepted.

[5] A. Boularias, O. Kroemer, and J. Peters. Learning robot grasping from 3d images with markov random fields. In *IEEE/RSJ International Conference on Intelligent Robot Systems (IROS)*, 2011.

[6] Zhaopeng Chen, Neal Y. Lii, Thomas Wimboeck, Shaowei Fan, Minghe Jin, Christoph Borst, and Hong Liu. Experimental study on impedance control for the five-finger dexterous robot hand dlr-hit ii. In *IROS*, pages 5867–5874. IEEE, 2010.

[7] Hao Dang and Peter K. Allen. Learning grasp stability. In *ICRA*, pages 2392–2397. IEEE, 2012.

[8] Renaud Detry, Carl Henrik Ek, Marianna Madry, Justus Piater, and Danica Kragic. Generalizing grasps across partly similar objects. In *IEEE International Conference on Robotics and Automation*, 2012.

[9] James J. Gibson. *The Ecological Approach To Visual Perception*. Lawrence Erlbaum Associates, new edition edition, September 1986.

[10] A. Herzog, P. Pastor, M. Kalakrishnan, L. Righetti, J. Bohg, T. Asfour, and S. Schaal. Learning of grasp selection based on shape-templates. *Autonomous Robots*, 2013.

[11] Tony Jebara and Risi Kondor. Bhattacharyya expected likelihood kernels. In *COLT*, volume 2777 of *Lecture Notes in Computer Science*, pages 57–71. Springer, 2003.

[12] Tony Jebara, Risi Kondor, and Andrew Howard. Probability product kernels. *J. Mach. Learn. Res.*, 5:819–844, December 2004.

[13] Robert Jenssen, Jose C. Principe, Deniz Erdogmus, and Torbjorn Eltoft. The cauchy-schwarz divergence and parzen windowing: Connections to graph theory and mercer kernels. *Journal of the Franklin Institute*, 343(6):614–629, 2006.

[14] Yun Jiang, Marcus Lim, Changxi Zheng, and Ashutosh Saxena. Learning to place new objects in a scene. *I. J. Robotic Res.*, 31(9):1021–1043, 2012.

[15] Marek Sewer Kopicki, Sebastian Zurek, Rustam Stolkin, Thomas Morwald, and Jeremy L. Wyatt. Learning to predict how rigid objects behave under simple manipulation. In *ICRA*, pages 5722–5729. IEEE, 2011.

[16] Hema Koppula and Ashutosh Saxena. Anticipating human activities using object affordances for reactive robotic response. In *RSS*, 2013.

[17] O. Kroemer, H. Ben Amor, M. Ewerton, and J. Peters. Point cloud completion using symmetries and extrusions. In *Proceedings of the International Conference on Humanoid Robots (HUMANOIDS)*, 2012.

[18] O. Kroemer, E. Ugur, E. Oztop, and J. Peters. A kernel-based approach to direct action perception. In *International Conference on Robotics and Automation (ICRA)*, 2012.

[19] Johannes Kulick, Tobias Lang, Marc Toussaint, and Manuel Lopes. Active Learning for Teaching a Robot Grounded Relational Symbols. In *International Joint Conference on Artificial Intelligence*, Beijing, China, 2013.

[20] L. Montesano, M. Lopes, A. Bernardino, and J. Santos-Victor. Modeling affordances using bayesian networks. In *Intelligent Robots and Systems, 2007. IROS 2007. IEEE/RSJ International Conference on*, pages 4102–4107, Oct 2007.

[21] Benjamin Rosman and Subramanian Ramamoorthy. Learning spatial relationships between objects. *I. J. Robotic Res.*, 30(11):1328–1342, 2011.

[22] Radu Bogdan Rusu and Steve Cousins. 3D is here: Point Cloud Library (PCL). In *IEEE International Conference on Robotics and Automation (ICRA)*, Shanghai, China, May 9-13 2011.

[23] E. Sahin, M. Cakmak, M. R. Dogar, E. Ugur, and G. Ucoluk. To Afford or Not to Afford: A New Formalization of Affordances Toward Affordance-Based Robot Control. *Adaptive Behavior*, 15(4):447–472, December 2007.

[24] Bernhard Schölkopf and Alexander J. Smola. *Learning with Kernels: Support Vector Machines, Regularization, Optimization, and Beyond*. The MIT Press, 1st edition, December 2001.

[25] K. Sjoo and P. Jensfelt. Learning spatial relations from functional simulation. In *Intelligent Robots and Systems (IROS)*, pages 1513–1519, Sept 2011.